Heterocyclic Letters
Vol. 9| No.2|149-164|Feb-April |2019
ISSN : (print) 2231–3087 / (online) 2230-9632
CODEN: HLEEAI
http://heteroletters.org

EXPEDIENT ACCESS TO 2,4,5-TRISUBSTITUTED IMIDAZOLES BY SIMPLE GRINDING USING KAOLIN IMPREGNATED ZnO/SiO_2 NANOCOMPOSITE: HOMO-LUMO, *IN VITRO* AND *INSILICO* STUDIES

Jayashree Avvadukkam[a], Narayana Badiadka[a]*, Sarojini B. Kunhanna[b]

[a]*Department of Studies in Chemistry, Mangalore University, Mangalagangothri-574 199, India*
[b]*Department of Industrial Chemistry, Mangalore University, Mangalagangothri-574 199, India*
**Corresponding author, E-mail: nbadiadka@yahoo.co.uk*

ABSTRACT
The convergent synthesis of 2,4,5-trisubstituted imidazole was studied using the newly introduced catalytic system of kaolin-impregnated ZnO/SiO_2 nanocompostite. The catalyst was effective enough to run the reaction under solvent-free conditions by grinding benzil, substituted benzaldehyde, substituted anilines, and ammonium acetate at room temperature. The characterization of synthesized catalyst by means of FESEM and XRD analysis revealed that the combination of the individual components retained its morphology and crystallinity. The HOMO-LUMO analysis has helped to understand the charge transfer within the molecules. The molecular docking studies showed that all newly synthesized molecules fit the active site of the β-Ketoacyl-acyl carrier protein synthase III enzyme (FabH) and represent a promising extension for the existing antibacterial agents.

KEYWORDS
Multicomponent, Kaolin-ZnO/SiO_2, Trisustituted imidazole, Molecular docking, HOMO-LUMO, *In vitro* studies

INTRODUCTION
Green chemistry has created a solid ground that provides essential design criteria for the development of efficient chemical synthesis of bulky privileged compounds.[i] The synthesis based on an environmentally friendly and efficient reusable catalyst and eliminating harmful solvents offers both economic and ecological benefits.[ii] Solvent free synthesis and multicomponent reactions are two important strategies that are gaining increasing attention .[iii] Research in multicomponent reactions (MCRs) with green chemistry is therefore important for the preparation of small molecule heterocyclic libraries and for drug discovery techniques.[iv] The next decade is likely to see a considerable evolution in this area.

Zinc oxide, a very economical, safe, and readily available Lewis acid catalyst, is widely used in organic synthesis and transformations.[v] It generally accepted that the blending two oxides that had little or no acidity, basicity and activity, resulted in a remarkable increase in these properties. This well proven in the case of ZnO which is an amphoteric metal oxide and SiO_2 which has a low acidity, a maximum acidity when these two are mixed in a 3:7 ratio.[vi] The efficiency of clay minerals to catalyze various organic reactions that occur on their surface and their interstitial space has been sought in recent years by synthetic chemists. The effectiveness of clay mineral as catalyst can be boosted by modifying its properties by incorporating various metal cations, molecules or complexes. Modifications usually lead to higher selectivity in product structure and yield. Kaolin is a white clay mineral with aluminosilicate structure and acidic nature which can be used as an efficient catalyst in variety of organic reactions.[vii] Incorporation of mixed ZnO/SiO_2 nanocomposite into calcined kaolin ends with a modified catalyst with high activity. In this work we have developed kaolin impregnated ZnO/SiO_2 nanocomposite and tested the efficiency of newly synthesized catalyst, by applied it to synthesize 2,4,5-tri substituted imidazoles *via* Radiszewski method. The Radiszewski synthesis is the most common route to 2,4,5-trisubstituted imidazoles recently observed, with condensation of benzil or benzoin, aldehyde, and ammonium acetate in the presence of various catalysts.[viii-xxiii] Past research on this are good in one way or another, but also with one or more disadvantages. The use of expensive reagents, long reaction time, complicated workup and purification, low yield, and generation of a large amount of toxic waste are some of the disadvantages that are commonly observed.

According to the World Health Organization (WHO), increasing antimicrobial infections and the limited number of antimicrobial drugs is one of the biggest threats people face worldwide. This highlights the need to develop new potent antibacterial drugs that researchers have focused on over the last decade.[xxiv] It is known that imidazole with suitable substitutions has a wide range of biological activities, especially in antimicrobial.[xxv-xxix] Drug discovery has seen a tremendous increase as technology evolves. The application of computational methods such as molecular docking, HOMO-LUMO analysis, etc. has shown the right path to synthesize compounds of pharmaceutical value and to screen the synthesized compounds based on activities. Herein, among the synthesized compounds, the newly synthesized 4 compounds were screened for antibacterial activity based on molecular docking by taking β-Ketoacyl-acyl carrier protein synthase III enzyme (FabH). The compounds were also tested for their antioxidant activity using DPPH radicals. HOMO-LUMO analysis of the compounds provided additional evidence for their biological activities.

RESULTS AND DISCUSSION

Characterization of catalyst

Micro structural and crystal structural examinations of newly synthesized catalyst were established by FESEM and XRD analysis respectively.

Field Emission Scanning Electron Microscopy (FESEM)

FESEM image provided a conception about surface morphology of synthesized nanocomposite. **Figure-I** shows FESEM image of synthesized nanocomposite. Equal distribution of flake like nanoparticles is visible in **Figure-Ia** which is an indication of the shape equality and homogeneity of the nanoparticles in their combined state. Crowded nanoparticles are clearly visible in **Figure-Ib** where the distinction of each nanoparticle has become difficult due to their ideal shape and proper mixing. Moreover agglomeration of nanoparticles is not observed since the particles are appearing as separable from one another.

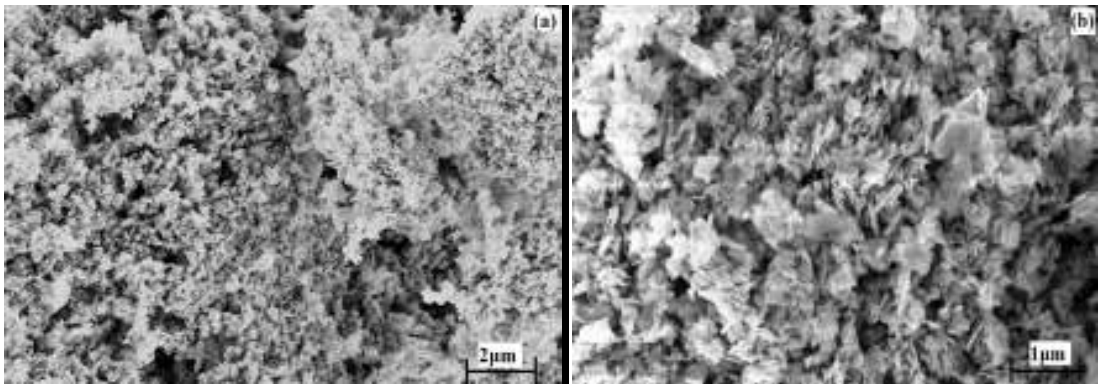

Figure-I FESEM image of Kaolin-ZnO/SiO_2 under the maginification of (**a**) 10 KX and (**b**) 40 KX.

XRD Analysis

The powder XRD pattern of the catalyst Kaolin-ZnO/SiO_2 is shown in **Figure-II**. The crystalline nature of the present catalyst is due to the combination of highly crystalline ZnO, SiO_2 and kaolin.[xxx-xxxii] The sharp intense narrow peaks at 2 theta values ranging from 17-35º are an indication of the crystallinity of the individual components. Further narrow peaks extending beyond 35º are also an indication that the combination of the nanoparticles retained its crystalline nature.

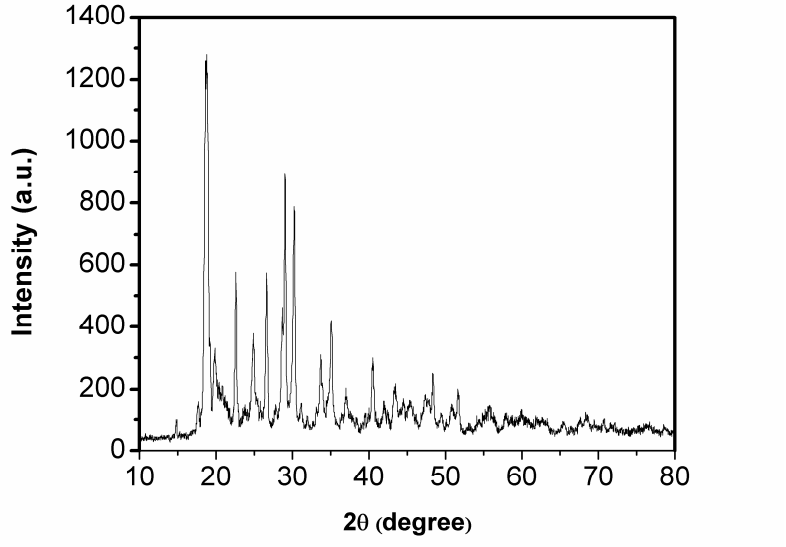

Figure-II XRD of Kaolin-ZnO/SiO_2

To optimize the reaction conditions, the reaction of 4-chlorobenzaldehyde, benzil and ammonium acetate was used as a model reaction. The effect of the amount catalyst on the product yield was tested and summarized in **Table-I & Figure-III**. The reusability of the catalyst was also examined under the optimized conditions, and the desired product was obtained in 95, 93, 91 and 90% yields after one to four runs, respectively (**Table-II & Figure-IV**). To test the efficiency of the synthesized catalyst, a comparative study was conducted with previous studies on the synthesis of 2,4,5-trisubstituted imidazoles (**Table-III**).

The schematic pathway for the synthesis of 2,4,5-trisubstituted imidazole is outlined in **scheme-I**. The substrate scope of the reaction was then evaluated by using a variety of structurally different aldehydes. The results obtained are shown in **Table-IV.**

Table-I Effect of increasing amount of catalyst on the preparation of desired products [a]

Entry	Catalyst (mmol)	Temperature (^{0}C)	Time	Yield[b] (%)
1	0	RT/Stirring	3 hrs	Trace
2	0.05	RT/Stirring	1.5 hrs	78
3	0.1	RT/Stirring	1 hrs	92
4	0.15	RT/Stirring	1 hrs	92
5	0.2[c]	RT Grinding	15 min	95
6	0.25	RT Grinding	15 min	95

[a] Reaction conditions: 4-chlorobenzaldehyde (1 mmol), benzil (1mmol) and ammonium acetate (1 mmol)
[b] Isolated yields
[c] Catalyst was reused four times

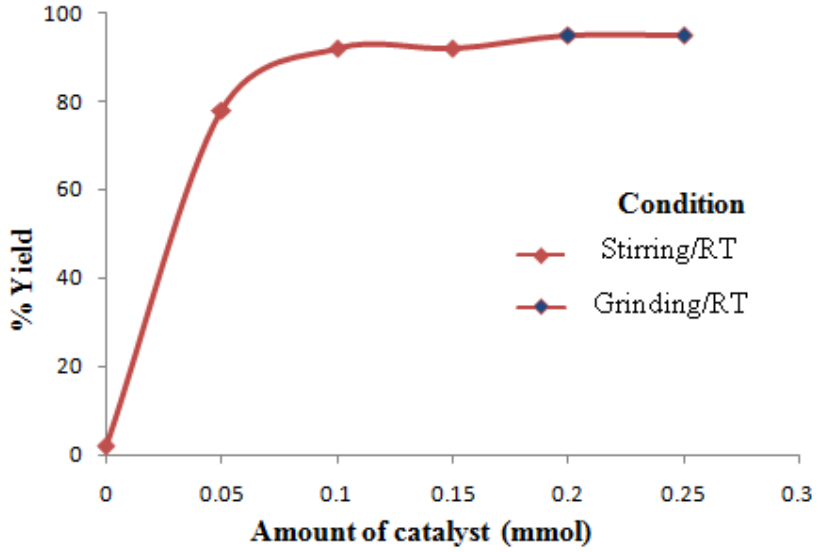

Figure-III Influence of the amount of catalyst on the product yield

Table-II Reusability and recyclability of Kaolin-ZnO/SiO_2 Catalyst

Entry	Number of runs	Yield (%)
1	1	95
2	2	93
3	3	91
4	4	90

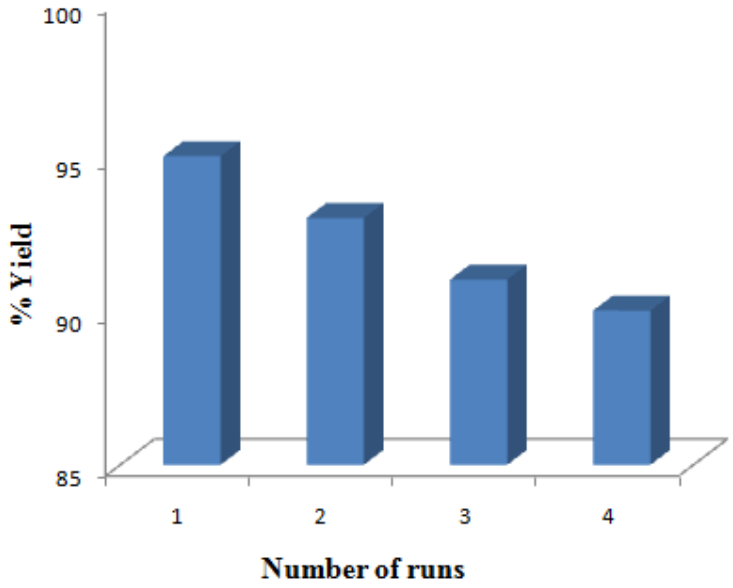

Figure-IV Reusability and recyclability of Kaolin-ZnO/SiO_2

Table-III Comparison of the efficiency of various catalysts in the synthesis of 2,4,5-trisubstituted imidazoles

Entry	Catalyst	Conditions	Time (min)	Yield (%)	[Ref]
1.	$InCl_3.3H_2O$	MeOH/RT	564	71	[8]
2.	L-proline	MeOH/60^oC	540	87	[9]
3.	KH_2PO_4	EtOH/Reflux	60	8	[10]
4.	Zr(acac)4	EtOH/Reflux	120	95	[11]
5.	$[(Et)_2NH_2^+]H_2PO_4^-$	Solvent free/100°C	15	96	[12]
6.	$Yb(OTf)_3$	AcOH/70^oC	120	83	[13]
7.	I_2	EtOH/75^oC	25	98	[14]
8.	$H_3[PW_{12}O_{40}]$	EtOH/Reflux	33	77	[15]
9.	$UO_2(NO_3)_2$ $6H_2O/Al_2O_3$	EtOH/Reflux	90	86	[16]
10.	[HeMIM]BF_4	MW	2.5	91	[17]
11.	Silica sulfuric acid	H_2O/Reflux	270	70	[18]
12.	[EMIM]OAc	EtOH/RT/Ultrasonic	90	96	[19]
13.	Trichloromelamine	Solvent free/110^oC	210	88	[20]
14.	ZnO	MeCN/RT	600	93	[21]
15.	$ZrCl_4$	MeCN/RT	64	89	[22]
16.	ZnO-SiO_2/Kaolin nanocomposite	Solvent free/Grinding	15	95	Present Work

The schematic pathway for the synthesis of 2,4,5-trisubstituted imidazoles is outlined in **scheme-I.**

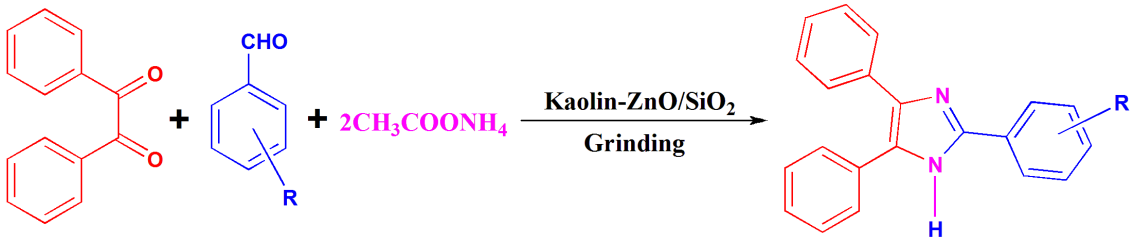

I **II** **III** **IVa-k**

Scheme-I Synthesis of 2,4,5-trisubstituted imidazole in presence of kaolin-ZnO/SiO_2 nanocomposite as catalyst.

Table-IV Synthesis of 2,4,5-trisubstituted imidazole derivatives in presence of kaolin-ZnO/SiO_2 nanocomposite as catalyst.

Entry	R	Product	Yield (%)/ Time (min)	Mp (^{0}C)		[Ref]
				Found	Reported	
1	4-H	4a	98/15	273-275	271-272	[12]
2	2-F	4b	96/15	170-172	172-174	[21]
3	2-Cl	4c	95/20	194-196	197-199	[20]
4	4-F	4d	96/15	193-195	190	[22]
5	4-Cl	4e	95/16	265-267	262-264	[12]
6	4-OH	4f	98/15	265-267	267-269	[12]
7	3,4-$(OCH_3)_2$	4g	96/15	212-214	210-212	[21]
8	3-Br-4-OCH_3	4h	95/16	234-236	-	-
9	4-SCH_3	4i	95/20	222-224	-	-
10	4-OC_4H_9	4j	96/15	232-234	-	-
11	3-OC_6H_5	4k	94/20	218-220	-	-

Structures of 2-(aryl)-4,5-diphenyl-1*H*-imidazoles were confirmed by their spectroscopic data. All the previously reported compounds (**4a-4g**) were confirmed by comparison of the reported melting point and characterized by ^{1}H NMR and mass spectra. The newly synthesized compounds (**4h-4k**) were characterized by FT-IR, ^{1}H NMR, ^{13}C NMR, mass spectra and elemental analysis. The IR spectrum of compound **4k** showed the presence of absorption band at 3304 cm^{-1} due to the NH group, at 2910 cm^{-1} due to the aromatic C-H stretching vibration, at 1336 cm^{-1} due to the =C-O-C stretching vibration. The ^{1}H NMR spectrum of **4k** showed a singlet at δ 12.64 ppm for NH. The aromatic phenyl protons appeared as a multiplet in the range of δ 8.10-6.97 ppm. In the ^{13}C NMR spectrum, signals due to aromatic carbons seen in the region of δ 157.5-115.4 ppm and methoxy carbon showed a signal at δ 55.5 ppm. The mass spectrum showed a deprotonated molecular ion peak at m/z 387 consistent with its molecular formula, $C_{27}H_{20}N_2O$.

It has been observed that the nature of substitution on aromatic aldehydes, *i.e.* electron-donating groups (eg. hydroxyl, methoxy) or electron-withdrawing groups (eg. halide) have no observable effect. The steric effect also has a traceable effect on the yield of the product. In general, the reactions were very simple, clean and no by-products were found.

***In silico* Molecular docking studies**

Molecular docking plays a pivotal role in structure based drug discovery by modeling putative interactions between small molecule and protein in different conformations and orientations. This provides an efficient and clear way to screen molecules for activity studies without any ambiguity. In this work, we performed molecular docking studies to examine and elucidate the newly synthesized molecules for their potential antibacterial activity.[xxxiii]

The putative interaction of the newly synthesized compounds **4h, 4i, 4j** and **4k** with active site of β-Ketoacyl-acyl carrier protein synthase III enzyme (FabH) (PDB ID: 1HNJ) is shown in the **Figure-V**. 2D models of ligands in the active site of β-Ketoacyl-acyl carrier protein synthase III is shown in the **Figure-VI**. FabH is condensing enzyme which plays key role in fatty acid biosynthesis and prime representative of antibacterial target drugs. The three dimensional structure of *Escherichia coli* FabH was refined to 1.46 A^o resolution. The docking of the ligands with target protein FabH showed that all the ligands exhibits sufficient interactions with the active site of the target protein. The aminoacids of the target protein show good interactions with ligands, especially with **4k.** All the compounds show a pi cation interaction with Arg 249 of FabH and a pi-pi stacking interaction with Phe 213. The ligand **4k** makes an additional pi-cation interaction with Arg 13. Details of the XP docking studies are summarized in **Table-V**.

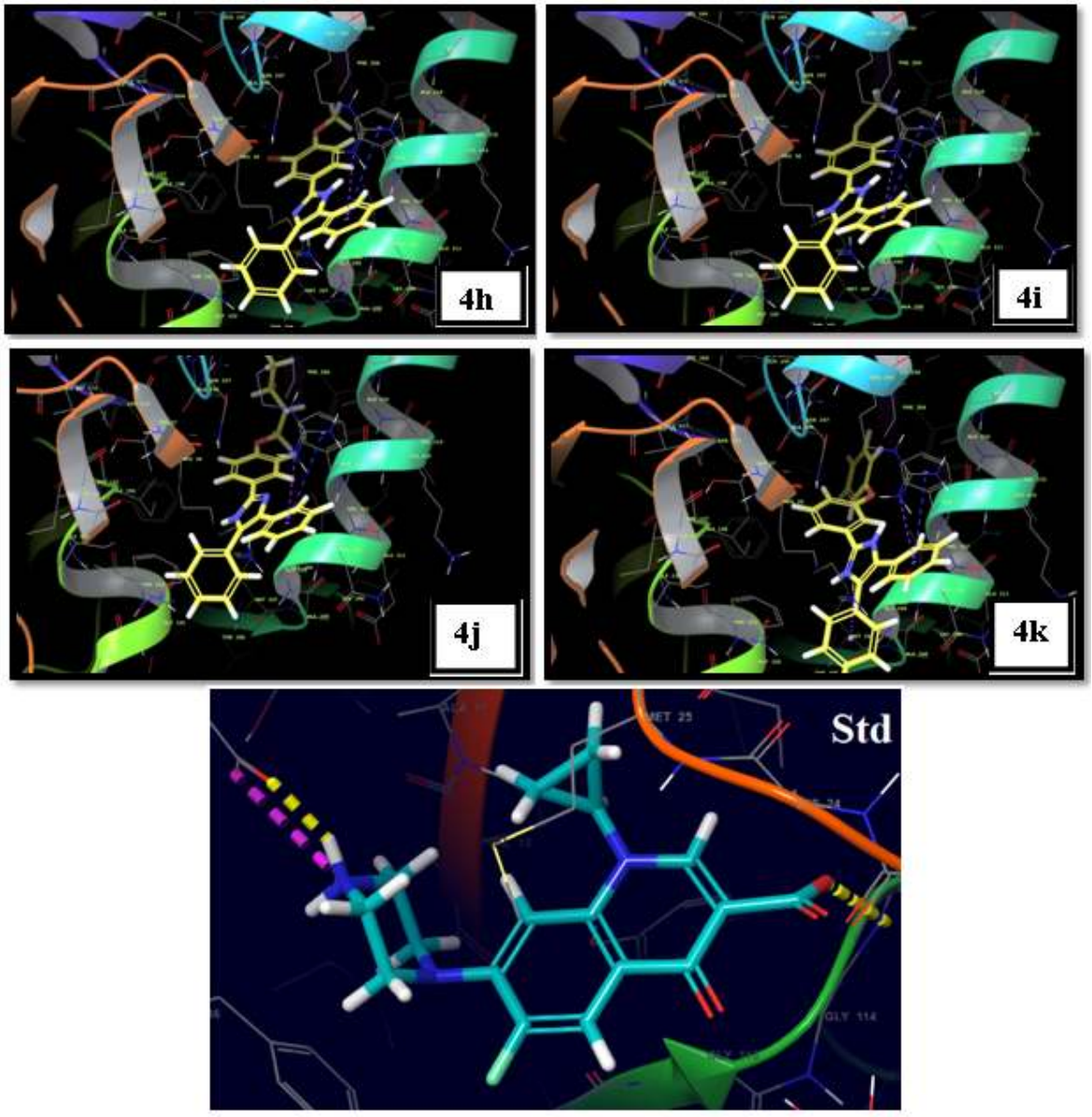

Figure-V β-Ketoacyl-acyl carrier protein synthase III-ligand interaction as visualized by maestro (version 10.5). The protein molecule is represented as ribbon. The interacting ligand and residues are represented as stick (Std- Ciprofloxacin)

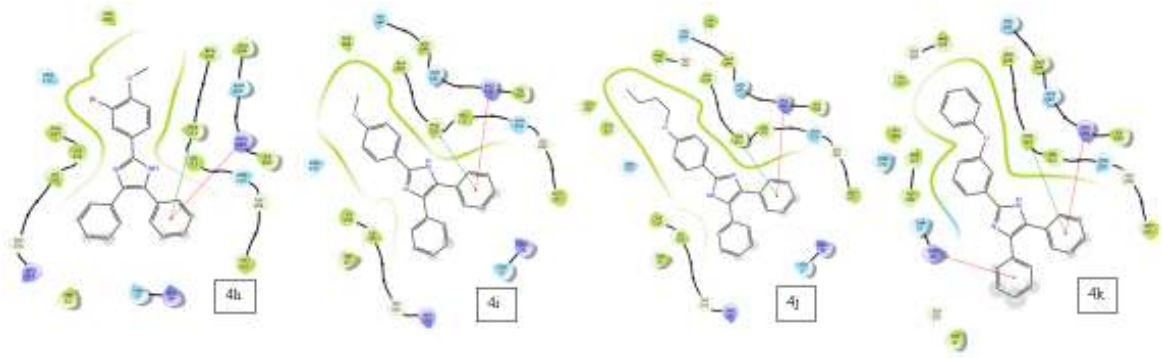

Figure-VI 2D models of ligands in the active site of β-Ketoacyl-acyl carrier protein synthase III

Table-V XP docking studies of **4h-4k** & Std. Ciprofloxacin

Entry	Compound	Docking Score (XP kcal/mol)	Glide gscore kcal/mol	Glide emodel kcal/mol
1	4h	-5.55	-5.554	-48.354
2	4i	-6.43	-6.436	-54.987
3	4j	-6.539	-6.543	-58.657
4	4k	-7.475	-7.481	-69.937
5	Std-Ciprofloxacin	-4.637	-4.637	-59.382

***In vitro* Antioxidant Assay Using DPPH Radical**

The % inhibition of the DPPH radical by the synthesized compounds is shown in the **Figure-VII**. The DPPH radical has an ability to react with hydrogen donors. The discoloration of the radical in the presence of a test compound determines its ability to scavenge free radicals thereby proving its antioxidant nature. Among the compounds tested however, only **4j** showed an inhibition of 79.25 ± 5.50 % during the initial screening. Upon conducting a detailed antioxidant evaluation, an IC_{50} value of 51 ± 4.22 µg/mL was observed.

***In vitro* Assay of Antimicrobial Activity**

The *in vitro* assay of anti-microbial activity is shown in the **Figure-VIII** for the four synthesized compounds. Based on the initial screening, the compound **4i** had an activity of 65.66 ± 3.51 %. The IC_{50} value of the compound was found to be 41.23 ± 2.41 µg/mL and MIC was found to be 102.75 ± 5.50 µg/mL. The anti-microbial activity of **4i** can be attributed to the presence of the sulfur atom in the structure and comparatively lower steric hindrance.

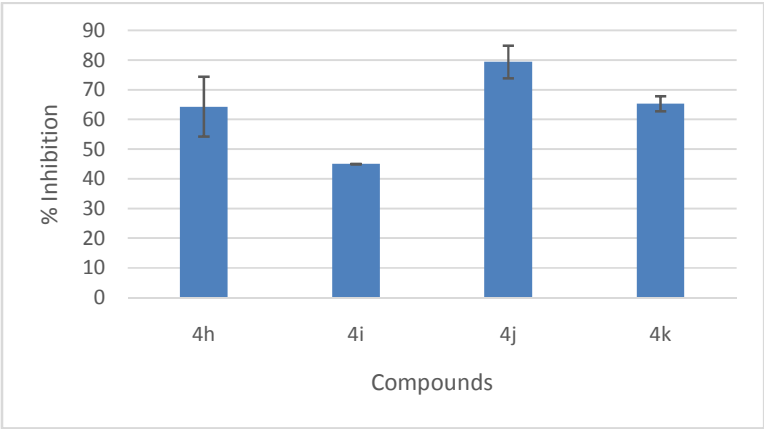

Figure-VII Antioxidant efficacy

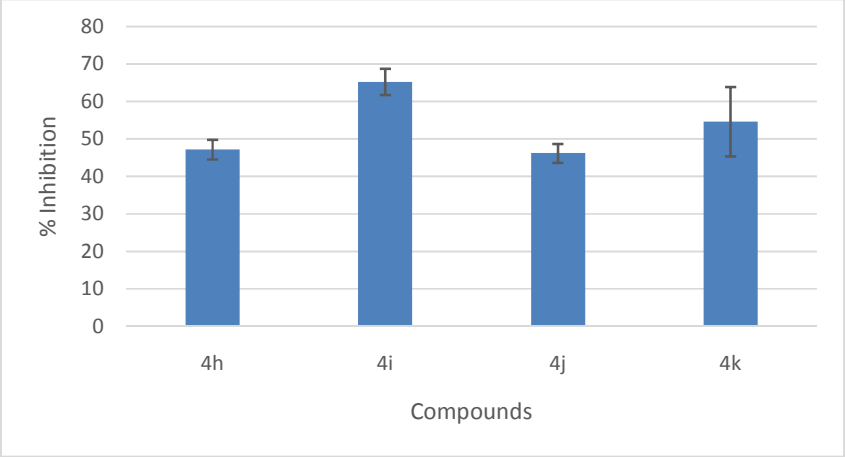

Figure-VIII Antimicrobial efficacy

Frontier Molecular Orbital analysis

Frontier molecular orbital analysis is a powerful model for assigning chemical reactivity and focuses primarily on the highest occupied molecular orbital and lowest unoccupied molecular orbitals (HOMO and LUMO). The localization of electron density on HOMO is always important because the electrons in this orbital are freest to participate in reaction. Similarly frontier molecular orbital theory predicts the site where the lowest unoccupied molecular orbital is localized, which is the best site for the electrophiles. In this way FMO gives clear evidence for the ionization energy (I) and electron affinity (A) through HOMO and LUMO ($I= -E_{HOMO}$ and $A= -E_{LUMO}$). [xxxiv]

In addition the energy gap between HOMO and LUMO is directly give hardness of the molecule. The hardness has a direct proportional relationship with the energy gap between HOMO and LUMO. The hardness of the molecule is related to stability of the molecule. The equation $\eta = (E_{LUMO}-E_{HOMO})/2$ predicts the global hardness and the combination of ionization energy and electron affinity yields an electronic chemical potential, $\mu = -(E_{HOMO} + E_{LUMO})/2$. The softness of the molecule is given as the reciprocal of hardness, $\sigma = 1/\eta$. Global electrophilicity index can be found out using the equation $\omega = \mu^2 /2\eta$. This index is a direct measurement of stability in terms of energy when gathered an additional electronic charge from the environment. The calculated value global electrophilicity index is the direct insight into the biological activity of selected compounds. The calculated parameters for all four compounds were summarized in **Table-VI**.

Table-VI Calculated parameters for **4h-4k** using B3LYP function and 6-311G basis set.

Entry	Compound	I (eV)	A (eV)	η	σ	μ	ω
1	4h	5.48	1.13	2.18	0.46	3.31	2.51
2	4i	5.69	1.44	2.13	0.47	3.57	2.99
3	4j	5.67	1.30	2.19	0.46	3.49	2.78
4	4k	5.88	1.51	2.19	0.46	3.70	3.12

Two frontier molecular orbital *viz*. HOMO and LUMO were examined for the selected compounds (**Figure-IX**). The HOMO of all 4 compounds is mainly delocalized by one of the phenyl rings of the benzil and phenyl ring of the aldehyde and a little by the imidazole ring.

The LUMO of all compounds are mainly on the imidazole ring and phenyl ring of the aldehyde.

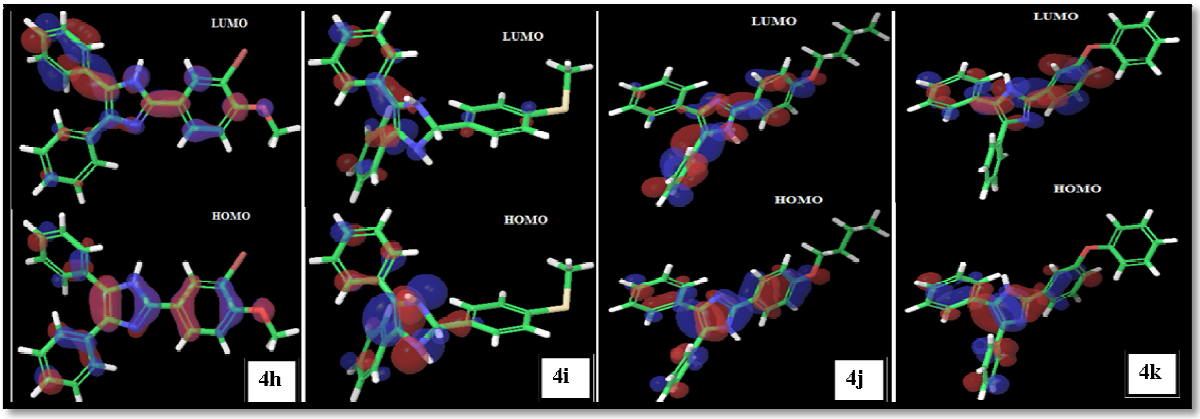

Figure-IX HOMO-LUMO plots of compound **4h, 4i, 4j and 4k**

Materials and Methods

General experimental conditions

All chemicals used were AR grades and were sourced from commercial suppliers. Purchased reagents used without further purification. Kaolin (Sigma-Aldrich) was dried at 120^{o}C in an oven. Microwave irradiation in the process of catalyst synthesis was conducted in a household LG microwave oven with continuous irradiation power of 0 to 500W. Powder XRD diffractogram of the catalyst was recorded on a bench top X-ray diffractometer, Rigaku MiniFlex 600 (Japan).The melting point was recorded in an open capillary tube and was uncorrected. All reactions and the purity of the compound were confirmed by thin layer chromatography using Merck silica gel 60 F_{254} coated aluminum plates using ethyl acetate and n-hexane as eluent. The spots were analyzed using a UV light detector chamber. The FT-IR spectrum was recorded on a Shimadzu FT-IR infrared spectrometer. The ^{1}H NMR spectrum (400 MHz) was recorded using Bruker Avance III 400 at a frequency of 400 MHz with TMS as the internal standard. The mass spectrum was obtained using a Shimadzu LCMS 8030 instrument. Elemental analysis was performed with Elementar Vario EL III C-H-N-Analyzer. X-ray diffraction data were collected on a Rigaku Saturn724 diffractometer using graphite monochromated Mo-Kα radiation at 296 K and complete data set was processed using Crystal Clear software. Ciprofloxacin and Quercetin was purchased from Sigma Aldrich, India.

Synthesis of kaolin impregnated ZnO/SiO_2 nanocomposite

Initially, ZnO nanoparticles were prepared according to the procedure described by Kumar et al.[xxxv] To an aqueous solution of zinc sulfate was added sodium hydroxide solution in 1: 2 molar ratios slowly with vigorous stirring. Stirring was continued for 10 hours and the resulting white precipitate was filtered and washed thoroughly with distilled water. The precipitate was then kept in the oven at 100 °C for 2 hours and finely pulverized using agate mortar. The powder was then calcined at 500 °C. The ZnO nanoparticles obtained by the above method were then mixed with silica gel in a molar ratio of 3:7. To this mixture, 5 ml of chloroform was added and stirred for 2 hours and subjected to microwave irradiation for 5 minutes. The resulting solid was mixed with 0.5 g of calcined kaolin and 5 ml of chloroform and stirred for 2 hours. The solid is then filtered using Whatman filter paper and dried in an oven at 100 °C. It is then calcined at 500 °C.

General procedure for the synthesis of 2,4,5-trisubstituted imidazoles by kaolin impregnated ZnO/SiO_2nanocomposite

A mixture of substituted benzaldehyde (1 mmol), ammonium acetate (2 mmol) and kaolin impregnated ZnO/SiO_2 nanocomposite was ground thoroughly with an agate mortar. To this mixture was added 1 mmol benzil and ground well for appropriate time (**Table-V**). The progress of the reaction was monitored by TLC. After completion of the reaction, the mixture was washed with distilled water and dried. The pure product was obtained by further recrystallization from ethanol.

2,4,5-Triphenyl-1*H*-imidazole (4a)

Pale yellow solid (0.68 g, 98%). mp: 273-275 ^oC; ^1H NMR (400 MHz, $CDCl_3$, δ ppm) δ: 12.67 (s, NH), 8.09 (d, J= 8.4 Hz, 3H) , 7.53-7.34 (m, 12H, Ar-H); MS, m/z: 296 [M^+].

2-(2-Fluorophenyl)-4,5-diphenyl-1*H*-imidazole (4b)

Pale yellow solid (0.66 g, 96%). mp: 170-172 ^oC; ^1H NMR (400 MHz, $CDCl_3$, δ ppm) δ: 12.57 (s, 1H, NH), 8.01 (t, J= 8.0 Hz, 1H), 7.54-7.21 (m, 13H, Ar-H); MS, m/z: 313 [M^+-H].

2-(2-Chlorophenyl)-4,5-diphenyl-1*H*-imidazole (4c)

Yellow solid (0.65 g, 95%). mp: 194-196 ^oC; ^1H NMR (400 MHz, $CDCl_3$, δ ppm) δ: 12.48 (s, 1H, NH), 7.96 (dd, J= 7.6 Hz, 1.6 Hz, 1H), 7.80 (dd, J= 8.0 Hz, 0.8 Hz, 1H), 7.74 (ddd, J= 7.2 Hz, 1.2 Hz, 1H), 7.66 (ddd, J= 8.4 Hz, 1.2 Hz, 1H), 7.56-7.48 (m, 10H, Ar-H); MS, m/z: 331 [M^+], 329 [M^+-2H].

2-(4-Fluorophenyl)-4,5-diphenyl-1*H*-imidazole (4d)

Pale yellow solid (0.66 g, 96%). mp: 193-195 ^oC; ^1H NMR (400 MHz, $CDCl_3$, δ ppm) δ: 12.64 (s, NH), 8.28 (m, 2H, Ar-H), 7.56-7.41 (m, 12H, Ar-H); MS, m/z: 315 [M^++H].

2-(4-Chlorophenyl)-4,5-diphenyl-1*H*-imidazole (4e)

Pale yellow solid (0.65 g, 95%). mp: 265-267 ^oC; ^1H NMR (400 MHz, $CDCl_3$, δ ppm) δ:12.67 (s, NH), 8.25 (d, J= 8.4 Hz, 2H), 7.76 (d, J= 8.8 Hz, 2H), 7.57-7.47 (m, 10H, Ar-H); MS, m/z: 331 [M^+], 329 [M^+-2H].

4-(4,5-Diphenyl-1*H*-imidazol-2-yl)phenol (4f)

Pale yellow solid (0.68 g, 98%). mp: 265-267 ^oC; ^1H NMR (400 MHz, $CDCl_3$, δ ppm) δ: 12.41 (s, NH), 9.75 (s, OH), 7.90 (d, J= 8.8 Hz, 2H), 7.53-7.21 (m, 10H, Ar-H), 6.86 (d, J= 8.8 Hz, 2H); MS, m/z: 312 [M^+].

2-(3,4-Dimethoxyphenyl)-4,5-diphenyl-1*H*-imidazole (4g)

Yellow solid (0.66 g, 96%). mp: 212-214 ^oC; ^1H NMR (400 MHz, $CDCl_3$, δ ppm) δ: 12.30 (s, NH), 7.64 (d, J=1.6 Hz, 1H), 7.52 (d, J= 7.2 Hz, 1H), 7.37-7.29 (m, 10H, Ar-H), 7.07 (d, J= 8.0 Hz, 1H), 3.85 (s, 3H, OCH_3), 3.81 (s, 3H, OCH_3); MS, m/z: 356 [M^+].

2-(3-Bromo-4-methoxyphenyl)-4,5-diphenyl-1*H*-imidazole (4h)

Pale yellow solid (0.65 g, 95%). mp: 234-236 ^oC; FT-IR (cm^{-1}): 3312 (N-H stretch), 2924 (Ar C-H stretch), 1218 (C-Br stretch); ^1H NMR (400 MHz, $CDCl_3$, δ ppm) δ:12.66 (s, NH), 8.02 (d, J= 2 Hz, 1H), 7.79 (dd, J= 8.4 Hz, 1.6Hz, 1H), 7.49-7.22 (m, 10H, Ar-H), 6.91 (d, J= 8.8 Hz, 1H), 3.88 (s, 3H, OCH_3): ^{13}C NMR: (100 MHz, $CDCl_3$) δ: 157.9, 147.9, 134.0,133.8, 133.7, 129.6, 129.3, 128.7, 128.5, 127.5, 127.2, 126.9, 126.8, 125.7, 125.4, 118.6, 112.8 (Ar-C), 55.5 (OCH_3); MS, m/z: 404 [M^+-H], 406 [M^++H]; Anal. Calcd. For $C_{22}H_{17}BrN_2O$: C 65.20, H 4.23, N 6.91%. Found: C 65.22, H 4.226, N 6.89%.

2-(4-(Methylthio)phenyl)-4,5-diphenyl-1*H*-imidazole (4i)

Pale yellow solid (0.66 g, 95%). mp: 222-224 ^oC; FT-IR(cm^{-1}): 3312 (N-H stretch), 2910 (Ar C-H stretch), 1390 (CH_3 C-H bend); ^1H NMR (400 MHz, $CDCl_3$, δ ppm) δ:12.50 (s, NH), 8.23-7.20 (m, 14H, Ar-H), 3.33 (s, 3H, SCH_3); ^{13}C NMR (100 MHz, $CDCl_3$) δ:147.7, 136.8, 133.7, 130.3, 130.2, 128.5, 127.7, 127.7, 127.6, 127.5, 127.4, 127.4, 127.2, 126.9, 126.4 (Ar-

C), 14.9 (S-CH_3); MS, m/z: 342 [M^+]; Anal. Calcd. For $C_{22}H_{18}N_2S$: C 77.16, H 5.30, N 8.18%. Found: C 77.14, H 5.27, N 8.21%.

2-(4-Butoxyphenyl)-4,5-diphenyl-1-imidazole (4j)

Brown solid (0.67 g, 96%). mp: 232-234 ^oC; FT-IR(cm^{-1}): 3484 (N-H stretch), 2916 (Ar C-H stretch), 1270 (=C-O-C stretch); ^1H NMR (400 MHz, $CDCl_3$, δ ppm) δ: 12.51 (s, NH), 7.66-6.78 (m, 14H, Ar-H), 3.83 (t, J= 6.4 Hz, 2H, CH_2), 1.62 (quint, 2H, CH_2), 1.34 (m, 2H, CH_2), 0.81 (t, 3H, CH_3); ^{13}C NMR: 157.6, 148.0, 133.9, 133.5, 129.7, 129.1, 128.9, 128.6, 128.4, 128.2, 127.5, 127.3, 122.9, 115.1, 115.09 (Ar-C), 68.9 (CH_2), 32.0 (CH_2), 19.3 (CH_2), 14.3 (CH_3); MS, m/z: 368.45 [M^+]; Anal. Calcd. For $C_{25}H_{24}N_2O$: C 81.49, H 6.57, N 7.60%. Found: C 81.47, H 6.54, N 7.62%.

Computational screening by molecular docking studies

Ligand preparation

Chemical structure of designed ligands **4h-4k** were drawn using 2D chem sketch of maestro (Version 11.5) and LigPrep tool was used for further optimization of ligand which produced 3D structures with lowest energies.[xxxvi]

Protein preparation and Grid generation

The three dimensional crystal structure of beta-ketoacyl-acyl synthase III complexed with Malonyl CoA (PDB ID: 1HNJ) with resolution of 1.46 Å was directly obtained from the Protein Data Bank (http://www.rcsb.org/pdb). During the process of protein preparation missing side chain loops of the proteins and missed residues were filled using prime tool. All the heteroatoms and water molecules were removed and the protein was further refined by restrained optimization. A receptor grid was generated on the protein obtained after restrained optimization.[xxxvii]

Ligand docking

Docking of optimized ligand analogues was done using Glide^{TM} program from schrodinger. Glide TM identifies predominant interactions between optimized ligand and a receptor. Glide docking was performed both in standard precision (SP) and extra precision (XP).[xxxviii]

Anti-oxidant studies

The synthesized compounds were evaluated for their anti-oxidant activity using 2,2-diphenyl-1-picrylhydrazyl (DPPH) free radical scavenging assay. The procedure was followed as per the reported literature with slight modifications.[xxxix, xl] Briefly, the compounds were solubilized in methanol (100 µg/mL for **4h, 4i and 4k**, and 125 µg/mL for **4j**). DPPH was dissolved in methanol (1 mmol/L) and subsequently added (100µL) to the above solutions (100 µL) in a microtitre plate. After incubation for 30 min in the dark, the absorbance of the samples was read using a microplate reader (BioTEK ELx800) at 517 nm. The % inhibition of DPPH was calculated considering the inhibition by the standard quercetin to be 100%. The compounds that showed a % inhibition for > 75 % was then incubated at different concentrations (5, 10, 25, 50, 75, 100 and 125 µg/mL) with DPPH reagent and the IC50 value was calculated.

% Inhibition of DPPH = $(Q_{ab} – S_{ab})/Q_{ab}$ * 100

Where, Q_{ab} and S_{ab} are the absorbance's of standard quercetin and sample respectively.

Anti-microbial studies using Resazurin microtitre assay

The anti-microbial property of the synthesized compounds was evaluated on the microbiological strains of S. aureus (MTCC number 96). The microorganism was cultured in Nutrient Broth medium at 37 ± 2°C. The protocol for the resazurin assay was followed as per the reported method with slight modifications. [xli] The stock solutions (100 µg/mL) of the four compounds were prepared in DMSO (0.9 % v/v) and ciprofloxacin was used as a standard antibiotic. The microbial culture was diluted to 0.5 MacFarland solutions to approximately

contain 1.5 X 10^6CFUs/mL. The strains (10 µL) were incubated with 25µL of the stock solutions and Nutrient Broth (150 µL). After incubation for 18 to 24 h, resazurin indicator in water(270 mg/ 40mL; 15µL) was added to the plates and incubated for 1 – 2 h. The color change of the indicator from purple to pink or colorless was taken as the positive reaction. The absorbance's were measured using the microplate reader at 540 nm in comparison to the standard ciprofloxacin. The compound showing a % inhibition of >65 % was then evaluated in a same procedure as above in varying concentrations in the range of 2 – 100 µg/mL. The IC50 value was obtained in a similar way as described in the Antioxidant study. The lowest concentration in which the change of color of the indicator was considered as the MIC value.

CONCLUSION

In summary, we have described the synthesis and characterization of a new catalytic system of mixed ZnO/SiO_2 nanocomposite impregnated calcined kaolin and used it for the synthesis of 2,4,5-substituted imidazoles. The catalyst was characterized by SEM and XRD analysis and all the new compounds were characterized by FT-IR, ^{1}H NMR, ^{13}C NMR, mass spectra and elemental analysis. The catalyst was efficient to allow the reaction by simple grinding at room temperature. The catalyst was able to recycle and reused for up to four cycles without much reduction in product yield. Excellent yields, environmentally friendly procedure, short reaction times, simple work-up procedure, and easy isolation are some of the other advantages of this method. Therefore, it is a useful supplement to the existing methods. Considering the fact that there are limited drugs available to combat the emerging microbial infections; the synthesized new compounds were tested for their antimicrobial activity based on molecular docking. Docking of targeted ligands with β-ketoacyl-acyl-carrier-protein synthase III enzyme (FabH) showed that all compounds show a fairly good interaction with the active site of receptor protein. These ligands were further tested for antimicrobial activities and an antioxidant assay using DPPH radicals. The HOMO-LUMO analysis of the compound was also performed, which gave insight into the charge transfer within the molecules.

ACKNOWLEDGMENTS

The authors thank the University Grants Commission, New Delhi, for their financial support from the Senior Research Fellowship and the one-time support from BSR for the purchase of chemicals. Authors thank DST-PURSE Lab, Mangalore University, for LCMS and SEM analysis.

CONFLICT OF INTEREST The authors declare that they have no conflict of interest.

REFERENCES

i. Cioc R. C., Ruijter E. and Orru R. V. A.; Green Chem., 16, (2014), 2958.
ii. Maleki A., Alirezvani Z. and Maleki S.; The 18th International Electronic Conference on Synthetic Organic Chemistry (2014) DOI: 10.3390/ecsoc-18-a003
iii. Jad Y. E., Gudimella S. K., Govender T., de la Torre B. G. and Albericio F.; ACS Comb Sci., 20, (2018) 187.
iv. Weber L.; Drug Discov Today 7, (2002), 143.
v. Bahrami K., Khodaei M. M. and Nejati A.; Monatsh Chem., 142, (2011), 159.
vi. Sumiyoshi T., Tanabe K. and Hattori H.; J Jpn Petrol Inst., 17, (1975), 65.
vii. Khaleghi S., Derikv F. and Heravi M. M. Iran JOC. 3, (2009), 194.
viii. Sharma S.D., Hazarika P. and Konwar D.; Tetrahedron Lett., 49, (2008), 2216.
ix. Samai S., Nandi G. C., Singh P. and Singh M. S.; Tetrahedron, (2009), 10155.
x. Joshi R. S., Mandhane P. G., Shaikh M.U., Kale R. P. and Gill C. H.;

Chin Chem Lett., 21 (2010) 429.
xi. Khosropour A.R.; Ultrason Sonochem., 15, (2008) 659.
xii. Marzouk A. A., Abbasov V. M., Talybov A. H. and Mohamed S. K. World J. Org Chem. 1, (2013), 6.
xiii. Wang L-M., Wang Y-H., Tian H., Yao Y-F., Shao J-H. and Liu B.; J Fluorine Chem., 127, (2006) 1570.
xiv. Kidwai M., Mothsra P., Bansal V., Somvanshi R. K., Ethayathulla A. S., Dey S., Singh T. P. J Mol Catal., 265, (2007), 177.
xv. Heravi M. M., Derikvand F. and Bamoharram F. F.; J Mol Catal. 263, (2007), 112.
xvi. Satyanarayana V. S. V. and Sivakumar A. Chemical Papers, 65, (2011), 519.
xvii. Xia M. and Lu Y. J Mol Catal., 265, (2007), 205.
xviii. Shaabani A. and Rahmati A.; J Mol Catal., 249, (2006), 246.
xix. Zang H., Su Q., Mo Y., Cheng B-W and Jun S.; Ultrason Sonochem., 17, (2010), 749.
xx. Mirjalili B. F., Bamoniri A. and Mohaghegh N. Curr Chem Lett., 2, (2013), 35.
xxi. Bandgar B. P., Hote B. S., Korbad B. L. and Patil S. A.; E-J Chem., 8, (2011), 1339.
xxii. Sharma G. V. M., Jyothi Y. and Lakshmi P. S.; Synth Commun 36, (2006) 2991.
xxiii. Karimi A. R., Alimohammadi Z., Azizian J., Mohammadi A. A. and Mohammadizadeh M. R.; Catal Commun., 7, (2006), 728.
xxiv. Tomi I. H. R., Al-Daraji A. H. R., Abdula A. M. and Al-Marjani M. F.; J Saudi Chem Soc., 20, (2016), S509.
xxv. Antolini M., Bozzoli A., Ghiron C., Kennedy G., Rossi T. and Ursini A.; Bioorg Med Chem Lett., 9, (1999), 1023.
xxvi. Jain A.K., Ravichandran V., Sisodiya M. and Agrawal R.K.; Asian Pac J Trop Med., 3, (2010), 471.
xxvii. Khan M. S., Siddiqui S. A., Siddiqui M. S. R. A., Goswami U., Srinivasan K. V. and Khan M. I. Chem Biol Drug Des., 72, (2008), 197.
xxviii. Husain A., Drabu S., Kumar N., Alam M. M. and Bawa S.; J Pharm Bioall Sci., 5 (2013), 154.
xxix. Sarala L., Merlin J. P. and Elanthamilan E.; J Chem Pharm Res., 8, (2016), 255.
xxx. Nandanwar R., Singh P. and Haque F. Z.; Am Chem Sci J., 5,(2015), 1.
xxxi. Kenne B. B. D., Elimbi A., Cyr M., Manga J. D. and Tchakoute H. K.; J Asian Ceram Soc., 3, (2015), 130.
xxxii. Talam S., Karumuri S. R. and Gunnam N. ISRN Nanotechnol (2012), Article ID 372505.
xxxiii. Vijesh A. M., Isloor A. M., Telkar S., Arulmoli T. and Fun H.-K.; Arab. J. Chem., 6 (2013), 197.
xxxiv. Panicker C.Y., Varghese H.T., Manjula P.S., Sarojini B.K., Narayana B. War J.A., Srivastava S.K., Alsenoy C. V. and Al-SaadA. A.; Spectrochim. Acta A. 151 (2015) 198.
xxxv. Kumar S. S., Venkateswarlu P., Rao V. R. and Rao G. N.; *Int Nano Lett*., 3, (2013), 30.
xxxvi. Schrödinger, L.L.C.; New York, (2016).
xxxvii. Jacobson M.P., Pincus D.L., Rapp C.S., Day T.J., Honig B., Shaw D.E. et al. Proteins: Structure, Function, and Bioinformatics. 55, (2004), 351.
xxxviii. Shivakumar D., Williams J., Wu Y., Damm W., Shelley J. and Sherman, W.; Journal of chemical theory and computation. 6, (2010), 1509.
xxxix. Sochor J., Ryvolova M., Krystofova O., Salas P., Hubalek J., Adam V., Trnkova L., Havel L., Beklova M., Zehnalek J., Provaznik I. and Kizek R.; Molecules, 15, (2010), 8618.

xl. Jadid N., Hidayati D., Hartanti S. R., Arraniry B. A., Rachman R. Y. and Wikanta W. AIP Conference Proceedings, (2017), 1854.
xli. Sarker S. D., Nahar L. and Kumarasamy Y. Methods, 42, (2007), 321.

Received on March 23, 2019.